SECOND EUROPEAN CONFERENCE ON EARTHQUAKE ENGINEERING
AND SEISMOLOGY, ISTANBUL AUG. 25-29, 2014

SYSTEM IDENTIFICATION OF THE E-DEFENSE FULL-SCALE FOUR STORY STEEL TEST STRUCTURE UTILIZING SHAKE TABLE TEST DATA

Roshanak OMRANI[1], Kazuhiko KASAI[2], Tuan Nam TRAN[3], Ralph E. HUDSON[4], Ertugrul TACIROGLU[5]

ABSTRACT

Acceleration data from a test structure are used to identify its lateral load-resistance properties through a time-domain parameter estimation algorithm. The specimen structure is a full-scale four-story moment resisting frame steel structure manufactured and tested at Japan's E-Defense testing facility. A series of shake table experiments were conducted in 2007 to excite the structure with scaled records of the 1995 Kobe earthquake. The structure was densely instrumented with accelerometers, strain gauges, and laser transducers, which collected adequate data for full characterization of the response history and the dynamic characteristics of the test structure.

The dense instrumentation array and the spatial completeness of the E-Defense test data offered an unprecedented opportunity to validate a recently proposed parameter estimation algorithm (Omrani et al., 2012a,b) that utilizes linear response histories for identifying stiffness and damping properties of shear-type building structures. The estimation algorithm is formulated in the time-domain and employs a least-squares-based methodology to extract the stiffness and damping matrices of individual stories of the test structure. The identified structural properties are subsequently used to extract modal properties of the structure for comparison with modal properties identified through conventional spectral analysis techniques.

INTRODUCTION

A series of pre-collapse and collapse tests were performed in 2007 at the Japan's E-Defense shake table facility to assess the performance of a specimen structure under scaled records of the JR Takatori recorded motion of the 1995 Kobe earthquake (Yamada et al., 2008; Suita et al., 2008). The test structure was a full-scale four-story steel moment resisting frame, which was designed according to Japan's building and seismic code specifications as noted by Yamada et al. (2008).

A 75-channel array with five tri-axial sensors at each level of the test structure and on the shake table was deployed to collect acceleration data during the pre-collapse tests. Force and deformation histories—deduced from column strain gauges and displacement wired sensors along the two lateral directions of the test structure—confirm that the response of the structure remained linear during the 20% Takatori excitation level (Fig.1). Therefore, the acceleration data from the aforementioned test is

[1] Assistant Project Scientist, University of California, Irvine, romrani@ucla.edu
[2] Professor, Tokyo Institute of Technology, Tokyo, kasai@serc.titech.ac.jp
[3] Graduate Student, Tokyo Institute of Technology, Tokyo, tuanam.t.aa@m.titech.ac.jp
[4] Research Scientist, University of California, Los Angeles, ralph@ucla.edu
[5] Professor, University of California, Los Angeles, etacir@ucla.edu

a suitable candidate to be used with a linear parameter estimation algorithm, which will be briefly described in the subsequent sections.

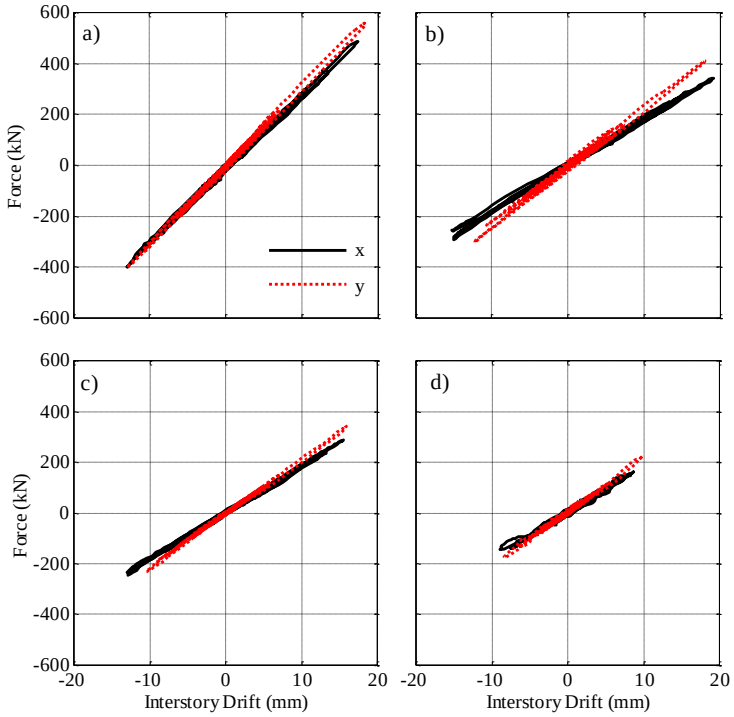

Figure 1. Shear Force (Evaluated from Column Strain) and Inter Story Drift (Measured by Wired Sensors) Relationships during the 20% Takatori Base Excitation, a)1st Story, b)2nd Story, c)3rd Story, d)4th Story

DESCRIPTION OF THE TEST STRUCTURE

The lateral load resisting system, as shown in Fig.2, consists of two-bay and single-bay moment resisting frames at the perimeter of each story along the longer and shorter dimensions of the structure, which are 10 m and 6 m, respectively. In addition to the peripheral frames, a single-bay frame at the centerline of each floor is aligned with the two other single-bay frames along the shorter dimension of the floor. Other than the seismic framing system, two additional floor beams in each direction contribute to the gravity load bearing of each floor. Non-structural components include ALC panels at the south, east, and west exteriors of the building, uniform floor slabs, two cantilevered slabs at the north exterior, dropped ceilings at the third and fourth stories, roof parapets, and a number of partition walls at the second, third, and fourth stories. Fig.3 illustrates the placement of tri-axial accelerometers for a general floor.

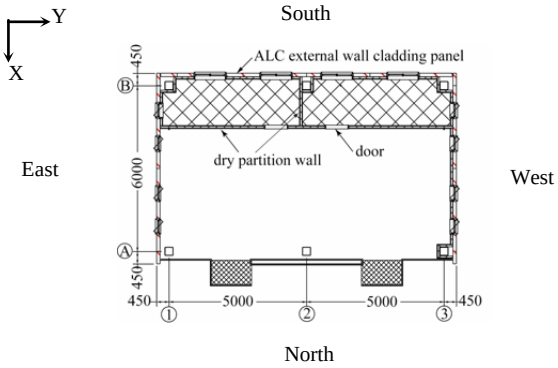

Figure 2. General Schematic View of Framing System and ALC Panels

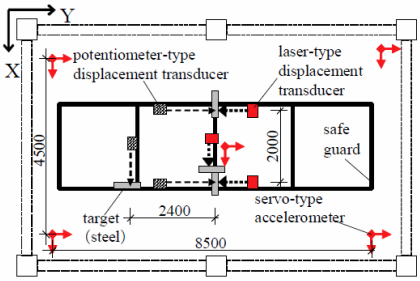

Figure 3. General Placement of Tri-axial Accelerometers

PARAMETER ESTIMATION METHODOLOGY

The parameter estimation algorithm employed here utilizes the equilibrium equations between story shear and restoring forces to identify the stiffness and damping matrices of individual stories in a shear-type building structure (Omrani et al., 2013a,b). Story shear is calculated as the cumulative summation of the inertial forces acting on the portion of the building which is above the story of interest—that is, for the i^{th} story, we have

$$\mathbf{k}_i\mathbf{u}_i + \mathbf{c}_i\dot{\mathbf{u}}_i = -\sum_{j=i}^{N} \mathbf{m}_j\ddot{\mathbf{x}}_j \tag{1}$$

where N denotes the total number of stories in the building. Matrices $\mathbf{k}$ and $\mathbf{c}$ correspond to the stiffness and equivalent viscous damping matrices of a single story and are defined as,

$$\mathbf{k} = \begin{bmatrix} k_{xx} & k_{xy} & k_{x\theta} \\ k_{yx} & k_{yy} & k_{y\theta} \\ k_{x\theta} & k_{y\theta} & k_{\theta\theta} \end{bmatrix}_i \qquad \mathbf{c} = \begin{bmatrix} c_{xx} & c_{xy} & c_{x\theta} \\ c_{yx} & c_{yy} & c_{y\theta} \\ c_{x\theta} & c_{y\theta} & c_{\theta\theta} \end{bmatrix} \tag{2}$$

The vector quantities $\mathbf{u}$ and $\ddot{\mathbf{x}}$ denote the interstory drift and absolute floor acceleration values, respectively, each comprising response quantities corresponding to two lateral and one torsioanl degrees of freedom, which characterize the idealized three-dimentional motion of the floor slabs in a shear-type building stucture. The story mass matrix $\mathbf{m}$ is defined as,

$$\mathbf{m} = \begin{bmatrix} m & 0 & -me_y \\ 0 & m & me_x \\ -me_y & me_x & I_o \end{bmatrix} \tag{3}$$

Lateral mass of story is shown with m. Parameters e_x, e_y, and I_o correspond to mass eccentricities and mass moment of inertia, which are evaluated with respect to the origin of an assumed coordinate system. Given mass properties and history of response, the 18 unknown elements of stiffness and damping matrices that are expanded in Eq.(2) can be estimated by fitting the unknown restoring forces to the measured story shear forces—at n time instants—by using Eq.(4) in a least-squares sense. That is,

$$\begin{bmatrix}\mathbf{k}_i & \mathbf{c}_i\end{bmatrix}_{3\times 6}\begin{bmatrix}\mathbf{u}_i(t)\\ \dot{\mathbf{u}}_i(t)\end{bmatrix}_{6\times n} = -\left[\sum_{j=i}^{N}\mathbf{m}_j\ddot{\mathbf{x}}_j(t)\right]_{3\times n} \quad (4)$$

The estimation algorithm relies on the full characterization of the in-plane rigid body motion of each floor. Therefore, the structure needs to be instrumented at each level with at least three lateral channels, from which lateral and torsional components of floor acceleration can be deduced. Considering the absence of permanent deformations due to the linearity assumption, the velocity and displacement histories can be calculated by integrating the recorded acceleration response.

PARAMETER ESTIMATION RESULTS

Direct least-squares estimation of the unknown parameters in Eq.(4) yields asymmetric stiffness and damping matrices, thus, violates the Maxwell-Betti Reciprocal Theorem. In order to circumvent such an outcome, the estimated matrices were symmetrized by averaging the off-diagonal elements. The symmetrized matrices were then used as the initial guess for an iterative constrained optimization problem that minimizes the norm of difference between the terms on the left- and right-hand sides of Eq.(5), while the off-diagonal elements (i.e., 12 out of the total 18 unknowns) were constrained to be equal in pairs, and the diagonal elements were constrained to be non-negative.

$$\begin{bmatrix}\mathbf{k}_i & \mathbf{c}_i\end{bmatrix}_{3\times 6}\begin{bmatrix}\mathbf{u}_i(t)\\ \dot{\mathbf{u}}_i(t)\end{bmatrix}_{6\times n}\begin{bmatrix}\mathbf{u}_i^{\mathrm{T}}(t) & \dot{\mathbf{u}}_i^{\mathrm{T}}(t)\end{bmatrix}_{n\times 6} = -\left[\sum_{j=i}^{N}\mathbf{m}_j\ddot{\mathbf{x}}_j(t)\right]_{3\times n}\begin{bmatrix}\mathbf{u}_i^{\mathrm{T}}(t) & \dot{\mathbf{u}}_i^{\mathrm{T}}(t)\end{bmatrix}_{n\times 6} \quad (5)$$

The identified values of lateral stiffness and viscous damping coefficients obtained through the constrained optimization are listed in Table 1 for the four stories of the test structure. The table also contains the analytical values of the lateral stiffness coefficients which have been taken equal to the slope of straight lines fitted to the force-deformation data of Fig.1. As expected, the estimated values of lateral stiffness reflect the contribution of non-structural elements, thus, are larger than the values that are calculated based on the amount of strain in the story columns.

Table 1. Story Lateral Stiffness Values and Coefficients of Viscous Damping

Story No.	k_{xx} (kN/m)		k_{yy} (kN/m)		c_{xx} (kN/m/s)	c_{yy} (kN/m/s)
	Estimated	Analytical	Estimated	Analytical	Estimated	Estimated
4	21770.14	18066.00	28017.72	20981.40	174.34	135.34
3	23296.09	18233.42	26843.82	20971.07	135.20	230.09
2	24625.48	18002.72	29407.90	22442.04	163.75	294.83
1	33439.80	28988.74	33528.92	31083.29	192.20	128.66

FREQUENCY-DOMAIN ASSESSMENT OF THE PARAMETER ESTIMATION RESULTS: DOMINANT PERIODS AND DAMPING RATIOS

The estimated stiffness matrices along with the known mass matrix of the structure are used for eigenvalue analysis, which yields the natural periods and mode shapes of the 12 analytical modes of vibration corresponding to the idealized shear building model. This is done by solving for the roots of the characteristic equation, in which **K** (assembled from the stiffness matrices of individual stories) and **M** correspond to the global stiffness and mass matrices of the shear building model, respectively, and ω is the circular frequency of vibration,

$$\det\left(\mathbf{K}-\omega^2\mathbf{M}\right)=0 \tag{6}$$

where

$$\omega=\frac{2\pi}{T} \tag{7}$$

The mode shape vector corresponding to the i^{th} natural period (T_i) is subsequently calculated by solving for the i^{th} eigenvector (ϕ_i) of matrix $\left(\mathbf{K}-\omega_i^2\mathbf{M}\right)$ through,

$$\left(\mathbf{K}-\omega_i^2\mathbf{M}\right)\phi_i=0 \tag{8}$$

Modal damping ratios are subsequently derived from the global damping matrix, **C**—which has been populated by the estimated damping matrices of individual stories—through orthogonal modal decomposition,

$$\zeta_i=\frac{\phi_i^{\mathrm{T}}\mathbf{C}\phi_i}{2\omega_i\left(\phi_i^{\mathrm{T}}\mathbf{M}\phi_i\right)} \tag{9}$$

The extracted modal properties are listed in Table 2 along with the properties identified through spectral analysis of the measured response. The mode shapes deduced from eigenvalue analysis are shown in Fig.4. As observed in Table 2, the estimated natural frequencies are in good agreement with the spectral analysis results. However, damping ratios obtained from modal decomposition of the estimated damping matrix are significantly larger than the damping ratios obtained through spectral analysis, particularly in higher modes.

Table 2. Natural Periods and Damping Ratios of the Idealized Shear Building Model

Mode	Eigenvalue and Modal Decomposition Analysis with Estimated Stiffness and Damping Matrices		Spectral Analysis	
	T (s)	ζ (%)	T (s)	ζ (%)
$x1$	0.823	2.5	0.825	2.1
$y1$	0.776	2.7	0.776	4.0
$\theta1$	0.670	1.3	-	-
$x2$	0.287	7.6	0.251	5.4
$y2$	0.267	6.6	0.246	6.9
$\theta2$	0.240	5.5	-	-
$x3$	0.185	11.5	-	-
$y3$	0.171	12.0	-	-
$\theta3$	0.150	6.2	-	-
$x4$	0.150	13.3	0.139	1.0
$y4$	0.139	18.9	0.130	1.3
$\theta4$	0.117	3.9	-	-

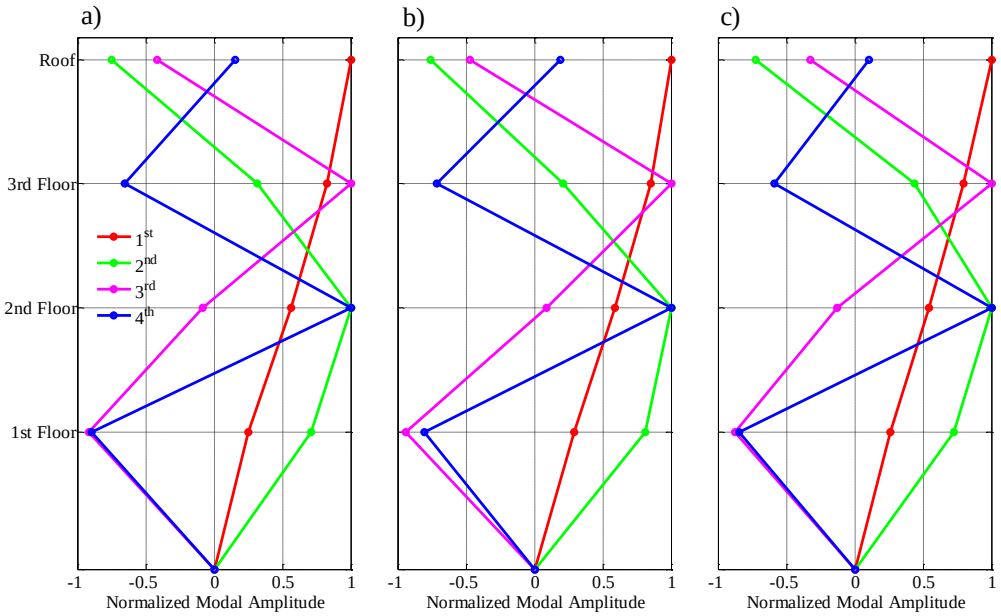

Figure 4. Mode Shapes from Eigenvalue Analysis of Estimated Stiffness Matrix of the Idealized Shear Building Model, a) Lateral *x*, b) Lateral *y* and, c) Torsional Modes

TIME-DOMAIN ASSESSMENT OF THE PARAMETER ESTIMATION RESULTS: SIMULATION OF STRUCTURAL RESPONSE

The identified story stiffness and damping matrices were assembled to form the global stiffness and damping matrices, which were subsequently employed for simulating response of the structure to 20% Takatori base excitation. Fig.5 and Fig.6 display measured and simulated absolute lateral floor accelerations. As demonstrated in the figures, the simulated response appears to be a low-pass filtered version of the measured response. This indicates that the higher modes are absent from the simulated response. Such an observation is consistent with modal decomposition of the estimated damping matrix in overestimating damping for higher modes of vibration. The overestimation of damping in lightly damped structures has been frequently reported in literature (see, for example, Juang and Longman, 1999) and devising numerical techniques for treating this issue is indeed a part of ongoing efforts relevant to the current study.

Another observation made here is the deterioration of the agreement between the simulated and measured responses of the first and second floors compared to the higher floors. This can be explained by comparing the modal contribution of the 1st and 4th normalized mode shapes at all floor levels, as done in Table 3 for the *x* lateral direction. Based on the values obtained for modal participation factors—given by Eq.(10), in which **L** is the influence matrix—the contribution of the first mode to the motion in the *x* direction is about 8 times the contribution of the last mode in the same direction.

$$\mathbf{\Gamma}_i = \frac{\boldsymbol{\phi}_i^{\mathrm{T}}\mathbf{L}\mathbf{M}}{\boldsymbol{\phi}_i^{\mathrm{T}}\mathbf{M}\boldsymbol{\phi}_i} \tag{10}$$

However, the modal contribution factors—i.e., the contribution of a mode to the response at a degree of freedom (Chopra, 2011)—are not uniform among all floors. The normalized modal amplitudes listed in Table 3 indeed correlate well with the modal contribution factors. Apparently, the 4th mode has higher contribution at the first and second floors relative to the upper floors. The columns labelled as "Modal Contribution" in Table 3 correspond to the product of modal participation factor with the modal amplitudes for each of the 1st and 4th modes. Note that this product is not the same as a modal contribution *factor*, but is a rough representation of its magnitude. The last column shows the

ratio between the contributions from the 4th and 1st modes at each floor level. At the two upper levels, contribution from the 4th mode is about 41% and 21% of contribution from the 1st mode. This ratio reduces to about 10% and 2% at the two lower floors. Therefore, overestimation of the damping ratio corresponding to the 4th mode has less severe effects on the simulated response at the two top floors, but drastically affects the simulated response of the first and second floors.

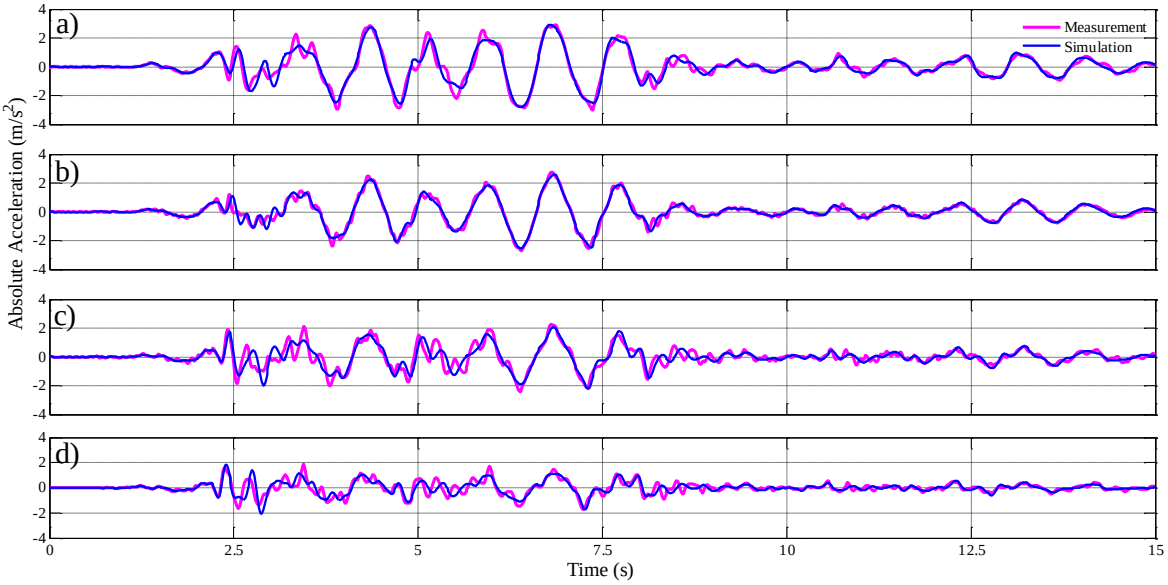

Figure 5. Comparison of Simulated and Measured Lateral Response in *x* Direction: a) Roof, b) 3rd Floor, c)2nd Floor, and d) 1st Floor

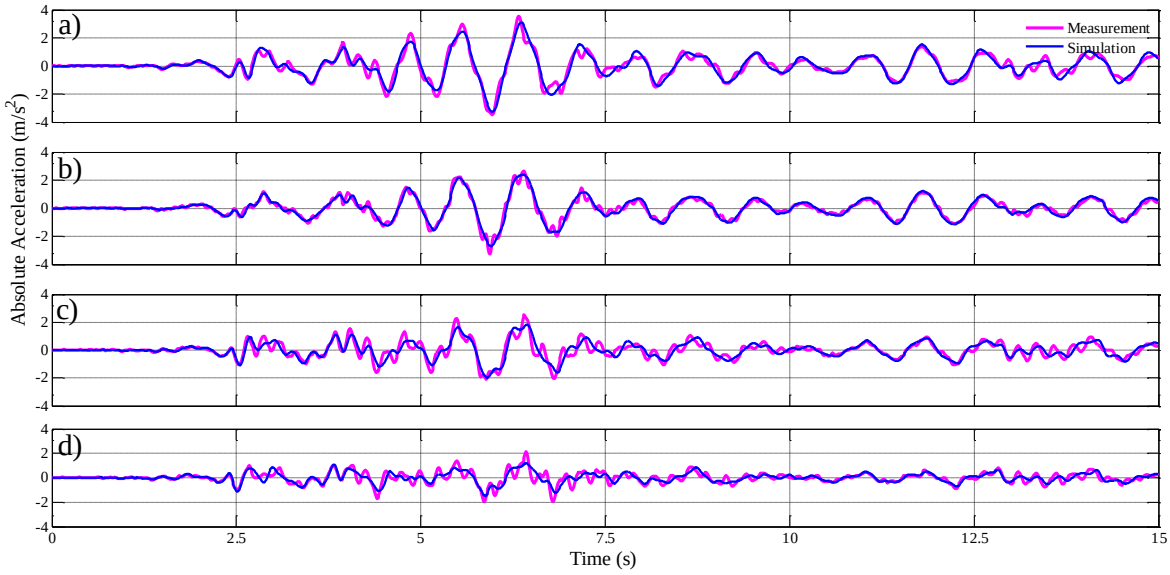

Figure 6. Comparison of Simulated and Measured Lateral Response in *y* Direction: a) Roof, b) 3rd Floor, c)2nd Floor, and d) 1st Floor

Table 3. Contribution of the 1st and 4th Modes of Vibration to Lateral Response in *x* Direction

Story No.	Normalized Modal Amplitude		Modal Participation Factor		Modal Contribution		(6)/(5) (%)
	1st Mode (1)	4th Mode (2)	1st Mode (3)	4th Mode (4)	1st Mode (1)×(3) (5)	4th Mode (2)×(4) (6)	
4	1.00	0.15	13.27	1.61	13.27	0.25	1.88
3	0.83	0.65			10.98	1.05	9.56
2	0.56	1.00			7.49	1.6	21.36
1	0.25	0.90			3.45	1.4	40.58

CONCLUSIONS

A constrained optimization time-domain parameter estimation technique was employed to identify the stiffness and damping matrices of individual stories of Japan's E-Defense full-scale four story steel moment resisting frame test structure, using vibration data from the 20% Takatori base excitation experiment. Natural periods and damping ratios were subsequently derived through eigenvalue analysis and orthogonal mode decomposition of the estimated matrices. Good agreement was observed between these natural frequencies and the ones obtained from spectral analysis of acceleration records. In general, the parameter estimation algorithm overestimated the damping characteristics of the structure. Discrepancies were observed between the damping ratios predicted through modal decomposition of the estimated damping matrix and those extracted by spectral analysis, particularly at higher modes of vibration. Simulation of structure's response with the identified stiffness and damping matrices yields results that are consistent with the overestimation of the damping ratios: higher modes of vibration are filtered from the simulated response. Fictitiously large damping of higher modes leads to more significant deviation of simulated response from the measured response at the two lower floors, where the contribution of higher modes is more dominant. Improvement of the numerical properties of the constrained optimization problem in order to circumvent identification of spuriously large damping properties is topic of future studies.

ACKNOWLEDGEMENT

The research reported herein was supported through the Collaborative Research Project-2013 sponsored by Materials and Structures Laboratory, Tokyo Institute of Technology. This support is greatly acknowledged. Any opinions expressed in this paper are those of the authors and do not necessarily reflect the views of sponsors.

REFERENCES

Omrani R, Hudson RE, Taciroglu E (2012a) "Story-by-story estimation of the stiffness parameters of laterally-torsionally coupled buildings using forced or ambient vibration data: I. Formulation & verification," *Earthquake Engineering & Structural Dynamics*, 41(12): 1609-1634

Omrani R, Hudson RE, Taciroglu E (2012b) "Story-by-story estimation of the stiffness parameters of laterally-torsionally coupled buildings using forced or ambient vibration data: II. Application to experimental data," *Earthquake Engineering & Structural Dynamics*, 41(12): 1635-1649

Yamada S, Suita K, Tada M, Kasai K, Matsuoka Y, Shimada Y (2008) "Collapse Experiment on 4-Story Steel Moment Frame: Part 1 Outline of Test Results", *Proceedings of The 14th World Conference on Earthquake Engineering*, Beijing, China, 12-17 October

Suita K, Yamada S, Tada M, Kasai K, Matsuoka Y, Shimada Y (2008) "Damage Collapse Experiment on 4-Story Steel Moment Frame: Part 2 Detail of Collapse Behaviour," *Proceedings of The 14th World Conference on Earthquake Engineering*, Beijing, China, 12-17 October

Juang JN and Longman RW (1999) Optimized system identification, NASA/TM-1999-209711, National Aeronautic and Space Administration, Langley Research Center, Hampton, Virginia

Chopra AK (2011) Dynamics of Structures: Theory and Application to Earthquake Engineering, 4th Ed., Prentice Hall, New Jersey